Role and Molecular Mechanisms of S100A9 Underlying Gemcitabine Chemoresistance in Bladder Cancer

KE MA AND HUI ZHANG*

Department of Urology, Shengjing Hospital of China Medical University, Shenyang, Liaoning Province 110000, China

Ma *et al.*: Mechanism of S100A9 Role in Gemcitabine Chemo Resistance

Bladder cancer cells become resistant to gemcitabine chemotherapy, S100A9 is involved in cancer progression and associated with chemo resistance, but the mechanism of S100A9's role in gemcitabine chemo resistance remains unknown. In this study, we investigated the role and mechanism of S100A9 in gemcitabine resistance in bladder cancer cells to provide a new therapeutic reference for gemcitabine resistance in bladder cancer cells. Induction of gemcitabine-resistant bladder cancer cells lines RT112, KU7, T24, lentiviral transfection of S100A9 in drug-resistant cells. 3-(4,5-dimethylthiazol-2-yl)-2,5 diphenyl tetrazolium bromide assay and clone formation assay were used to detect cell proliferation, transwell assay was used to detect cell migration and invasion, flow cytometry was used to detect apoptosis level, Western blot to detect apoptosis-related proteins and phosphatidylinositol-3-kinase/protein kinase B/mammalian target of rapamycin pathway. S100A9 transcription and translation levels were significantly elevated in gemcitabine-resistant bladder cancer cells compared with bladder cancer cells. Compared with the empty group, the si-S100A9 group showed a significant decrease in the survival rate of gemcitabine-resistant cells, a significant decrease in the levels of Bcl-2-associated X protein, cleaved caspase-3, phosphatidylinositol-3-kinase/protein kinase B/mammalian target of rapamycin protein, the number of clone formation, the number of cells migrating and invading. As well as a significant increase in the rate of apoptosis and the level of B-cell lymphoma 2 protein. Compared with the S100A9 group, the cell survival rate in gemcitabine-resistant bladder cancer cells were decreased in the S100A9+LY294002 group. S100A9 is highly expressed in gemcitabine-resistant bladder cancer cells; S100A9 promotes gemcitabine resistance in bladder cancer cells by targeting and excite the phosphatidylinositol-3-kinase/protein kinase B/mammalian target of rapamycin pathway.

Key words: S100A9, gemcitabine, chemoresistance, bladder cancer, phosphatidylinositol-3-kinase/protein kinase B signaling pathway

Bladder Cancer (BC) is a malignant tumor that occurs in the mucosa of the bladder and is the most common malignant tumor of the urinary system[1]. BC has a high rate of clinical recurrence, is a major global health concern, and has limited treatment options for advanced disease[2]. Metastasis and invasion of BC cells are major factors in tumor recurrence[3,4]. Chemotherapy remains a key therapeutic strategy, with GEM being a widely used and effective chemotherapeutic agent[5]. However, the emergence of chemo resistance poses a major challenge to successful BC treatment, leading to treatment failure and disease progression[6].

One of the molecular factors implicated in chemo resistance is S100A9, a member of the S100 calcium-binding protein family. S100A9 has been shown to play critical roles in various physiological and pathological processes, including inflammation, immune response, and cancer progression[7-9].

In recent years, accumulating evidence has suggested a potential involvement of S100A9 in mediating chemo resistance in different cancer types, including BC[10-12]. However, the precise molecular mechanisms by which S100A9 contributes to Gemcitabine (GEM) resistance in BC remain elusive, the role and mechanisms of S100A9-specific GEM chemo resistance in BC are poorly understood.

Many recent studies have found that S100A9 is closely associated with cell invasion and migration[9,13,14]. Moradpoor *et al.*[15] found S100A9

with frequent expression and enrichment of Phosphatidylinositol 3-Kinase (PI3K)-Protein Kinase B (Akt) signaling pathway in the invasive characterization of cancer cells. In addition many studies have confirmed that the mechanism of action of S100A9 is related to the PI3K-Akt signaling pathway[16-18]. Hence, understanding the role of S100A9 in GEM chemo resistance is of utmost importance in advancing our knowledge of BC biology and improving treatment outcomes.

Therefore, this study aims to investigate the role of S100A9 and unravel the underlying molecular mechanisms responsible for GEM chemo resistance in BC. To achieve this, we will perform *in vivo* experiments, evaluation of the role and mechanism of S100A9 in GEM-resistant BC cells using cell biology.

MATERIALS AND METHODS

Cell culture:

BC cell lines RT112, KU7, and T24 were purchased from American Type Culture Collection (ATCC), (Manassas, Virginia, United States of America (USA)). Briefly, all cells were cultured in Roswell Park Memorial Institute (RPMI) 1640 medium (Life Technologies) supplemented with 10 % Fetal Bovine Serum (FBS), (Hyclone Laboratories, South Logan, Utah, USA) in a humidified incubator containing 5 % of Carbon dioxide (CO_2) at 37°.

Drug-resistant cell construction:

BC cells in logarithmic growth phase were plated in 24-well plates, and the cells were first shocked with a high dose of GEM at 2 μmol/l. After 24 h of culture, the medium was replaced with normal medium, and the cells were allowed to recover. After 24 h of incubation, the medium was replaced with normal medium, and the dose of GEM was increased by a gradient of 0.02 μmol/l every 48 h. The maximum concentration of GEM that allowed the cells to grow continuously after the addition of GEM was taken as the optimal concentration, and the cells were stimulated with the optimal concentration for about 2 w to stabilize the cell passaging and be used for subsequent experiments.

Enzyme-Linked Immunosorbent Assay (ELISA):

The expression levels of S100A9 were measured using an ELISA (Abcam). Briefly, we diluted the standard, added the sample and enzyme to the test tube, and incubated at 37° for 10 min after which the reaction was stopped and the Optical Density (OD) was measured at 450 nm.

Quantitative Real-Time Polymerase Chain Reaction (qRT-PCR):

Total Ribonuclic Acid (RNA) of cancer cells was isolated from cells and qRT-PCR was carried out using the Trizol reagent (Invitrogen, Carlsbad, California, USA) according to the product instruction. Glyceraldehyde 3-Phosphate Dehydrogenase (GAPDH) was used as the control. The relative S100A9 expression was calculated by $2^{-\Delta\Delta CT}$ method. The primers used in this study were listed as follows; S100A9 forward 5'-TCCTCGGCTTTGACAGAGTG-3'; reverse 5'-GTCACCCTCGTGCATCTTCT-3'; GAPDH forward 5'-ACGGATTTGGTCGTATTGGGCG-3' and reverse 5'-GCTCCTGGAAGATGGTGATGGG-3'. The experiment was repeated three times in parallel.

Western blot assay:

Total proteins were extracted using radioimmunoprecipitation assay lysis buffer (Solarbio) and quantified using a bicinchoninic acid assay kit (Solarbio). 20 g of proteins were separated by sodium dodecyl sulfate-polyacrylamide gel electrophoresis (Solarbio) and transferred onto polyvinylidene fluoride membranes (Millipore, Massachusetts, USA). After blocking with 5 % skim milk, the membranes were incubated for 1 h at room temperature with primary antibodies against cleaved caspase-3, Bcl-2-Associated X Protein (BAX), B-Cell Lymphoma 2 (Bcl-2) and PI3K/AKT/mammalian Target of Rapamycin (mTOR) pathway. Beta (β)-tubulin was used as a control and all antibodies come from Abcam.

Lentiviral transfection:

$5×10^5$ cells were inoculated in 6-well plates 24 h before transfection. 100 pmol microRNA (miRNA) was diluted in 250 μl Opti-Minimal Essential Medium (MEM), and gently soiled for 5 times. Dilute 5 μl Lipofectamine® RNAiMAX in 250 μl Opti-MEM, then gently smooth it for 5 times, and let it stand for 5 min at room temperature. The two solutions were gently homogenized for 5 times and incubated at room temperature for 20 min to obtain the complex. 500 μl compound was added to the cells and the plates were shaken. After 4 h culture,

the new medium was replaced and cultured for 24 h to detect the expression of transferred genes. After transfection, the effect of small interfering RNA (siRNA) transfection was verified by RT-qPCR and ELISA, and the transfected cells were used for subsequent experiments.

Grouping:

Cells were divided into a blank group (no transfected), empty group (transfected empty vector), si-S100A9 group (drug-resistant cells transfected with lentivirus without S100A9), S100A9 group (drug-resistant cells transfected with lentivirus containing S100A9), and S100A9+LY294002 group (cells were treated with 10 µM LY294002 for 24 h).

3-(4,5-Dimethylthiazol-2-yl)-2,5 Diphenyl Tetrazolium Bromide (MTT) assay:

The cells (2×10^4 cells/well) were seeded into a 96-well plate. The proliferation of cancer cells was measured using the MTT according to the manufacturer's instructions. Viable cells were assessed by the absorbance at 490 nm using a microplate reader (Molecular Devices, Sunnyvale, California, USA).

Clone formation assay:

The cells (1×10^3 cells/well) were seeded into a 6-well plate. The clone of cancer cells was measured using the acetic acid according to the manufacturer's instructions. Clone cells were assessed by the absorbance at 492 nm using a microplate reader (Molecular Devices, Sunnyvale, California, USA).

Transwell assays:

Transwell assay was used to assess the ability of cell migration and invasion. Briefly, the Matrigel (Becton, Dickinson and Company, New Jersy, USA) was 1:4 diluted, and 100 µl of the dilution was coated on the upper surface of the transwell chamber at 37° overnight. The transfected cells were detached from the wells using enzyme, and then resuspended into 200 µl medium. The 100 µl cell suspension was added into the transwell chamber, and 700 µl of the medium containing 10 % FBS was added into the lower chamber of the 24-well plate. The bubbles were carefully avoided. After an incubation of 48 h, the transwell chamber was washed with Phosphate Buffer Saline (PBS) and then fixed with 4 % Paraformaldehyde (PFA)

for 20 min. After washing, cells were stained with 0.1 % crystal violet for 15 min. After washing, cells were photographed under a microscope (Nikon, Japan) and five areas were randomly selected for cell counting and measured.

Flow Cytometry (FCM) assay:

To evaluate the S100A9 on cell apoptosis of BC cells 5637 and T24, FCM assay were performed using Annexin V-Fluorescein Isothiocyante (FITC)/Propidium Iodide (PI) apoptosis detection kit (Beyotime Biotechnology, Shanghai, China) following the manufacturer's instructions. In concrete, 5637 and T24 were seeded into 6-well plates and transfected with interfering S100A9 or overexpressed-S100A9. The 5637 and T24 cells were collected for apoptosis analysis after transfected for 48 h, stained with (FITC)-Annexin V and PI. Finally, the apoptosis rate of cells was measured and analyzed by BD FACSCalibur™ (BD, USA).

Statistical analysis:

GraphPad Prism 8.0 software was used for the statistical analysis, and all data are presented as the mean±Standard Deviation (SD). Student's t-test was used for comparisons between two groups. One-way Analysis of Variance (ANOVA) followed by Tukey's post hoc test was used for the calculation of more than two independent groups. $p<0.05$ was considered statistically significant. All experiments were performed at least three times.

RESULTS AND DISCUSSION

To investigate the role of S100A9 in BC cells, we induced GEM resistance in BC cells (RT112-Gr, KU7-Gr and T24-Gr). By examining the expression levels of S100A9 messenger RNA (mRNA) and protein before and after GEM resistance in RT112, KU7, and T24 cells, we observed a significant increase compared to normal BC cells. The upregulation of S100A9 suggests its potential involvement in GEM resistance in BC cells. The results indicate that GEM resistance leads to an upregulation of S100A9 expression in BC cells. Consequently, we generated S100A9 overexpression and S100A9 knockdown in RT112-Gr, KU7-Gr, and T24-Gr cells using lentiviral transduction. After transfection, we assessed the expression levels of S100A9 in RT112-Gr, KU7-Gr, and T24-Gr cells using RT-qPCR and ELISA. Compared to the empty control group, the si-S100A9 group showed a

significant decrease in S100A9 mRNA and protein levels. Conversely, the S100A9 overexpression group exhibited a significant increase in S100A9 mRNA and protein levels (fig. 1). These trends were observed consistently in all three cell lines, indicating successful lentiviral interference of S100A9 in the cells.

We conducted MTT assays and clone formation assays to assess the proliferation of RT112-Gr, KU7-Gr, and T24-Gr cells after S100A9 lentiviral interference. As shown in fig. 2, compared to the empty control group, the si-S100A9 group in RT112-Gr cells exhibited a reduction in the number of cell clones, as well as a significant decrease in cell viability and optical density of the clones. Conversely, in the S100A9 overexpression group of RT112-Gr cells, there was an increase in the number of cell clones, along with a significant rise in cell viability and optical density of the clones. Similar results were observed in KU7-Gr and T24-Gr cells. In the si-S100A9 group, there was a decrease in the number of cell clones, as well as a significant reduction in cell viability and optical density of the clones. Conversely, in the S100A9 overexpression group, there was an increase in the number of cell clones, along with

a significant rise in cell viability and optical density of the clones. These results collectively demonstrate that interfering with S100A9 expression in GEM resistant cells can inhibit cell growth. We performed Western blot assays to evaluate the protein expression of cleaved caspase-3, BAX, and Bcl-2 in RT112-Gr, KU7-Gr, and T24-Gr cells after S100A9 lentiviral interference. As shown in fig. 3, in KU7-Gr, T24-Gr, and RT112-Gr cells, the si-S100A9 group exhibited a significant increase in the protein expression levels of cleaved caspase-3 and BAX, while the protein expression level of Bcl-2 significantly decreased compared to the empty control group. Additionally, in the S100A9 group, there was a significant increase in cleaved caspase-3 and BAX protein expression levels, and a significant decrease in Bcl-2 protein expression levels compared to the empty group. Furthermore, we detected cell apoptosis through FCM and found that the apoptosis rate was significantly increased in the si-S100A9 group, whereas it was significantly decreased in the S100A9 group compared to the empty group. These results collectively demonstrate that interfering with S100A9 expression in GEM-resistant cells can promote cell apoptosis.
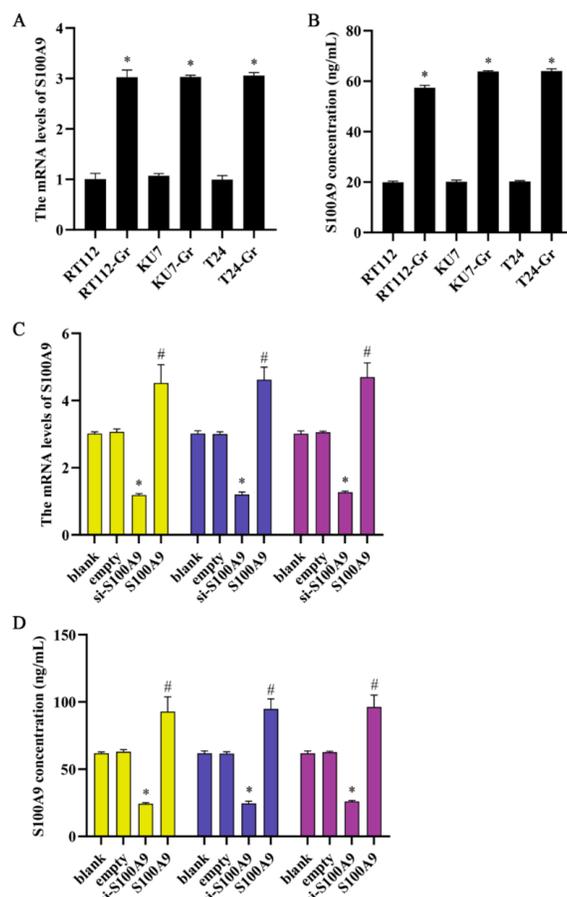

Fig. 1: S100A9 is highly expressed in GEM-resistant BC cells, (A): mRNA levels of S100A9 detected by qRT-PCR; (B): Protein levels of S100A9 detected by ELISA; (C): mRNA levels of S100A9 detected by qRT-PCR and (D): The protein levels of S100A9 detected by ELISA
Note: *p<0.05 *vs.* normal cell group and #p<0.05 *vs.* empty group, (▭): RT112-Gr; (▭): KU7-Gr and (▭): T24-Gr
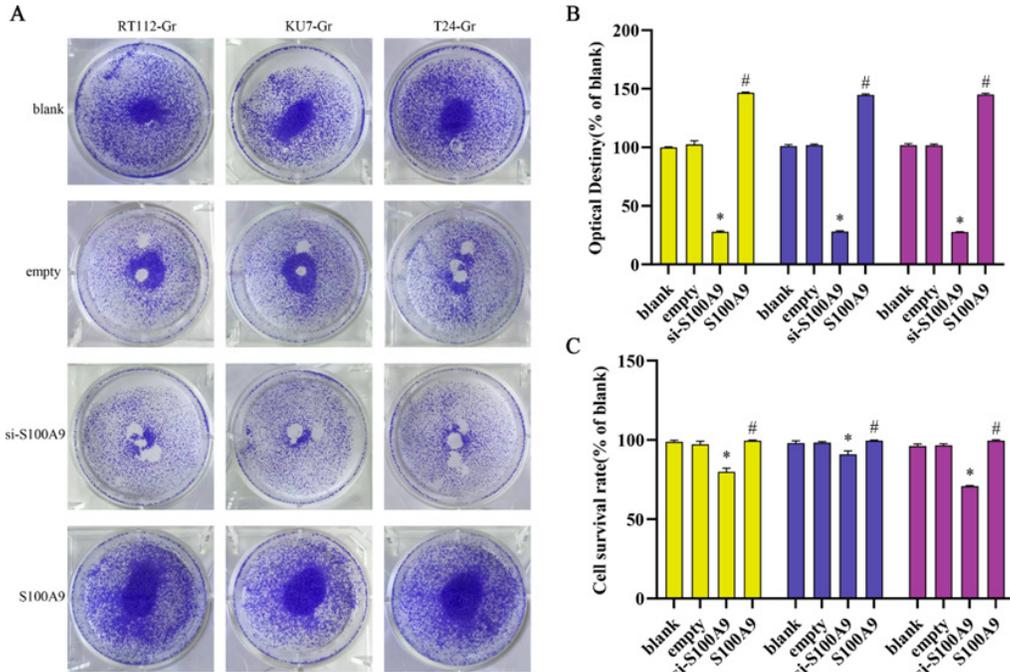
Fig. 2: The effect of S100A9 in GEM-resistant BC cells growth, (A and B): Clone formation assay and (C): MTT assay
Note: *p<0.05 *vs.* normal cell group and #p<0.05 *vs.* empty group, (▇): RT112-Gr; (▇): KU7-Gr and (▇): T24-Gr
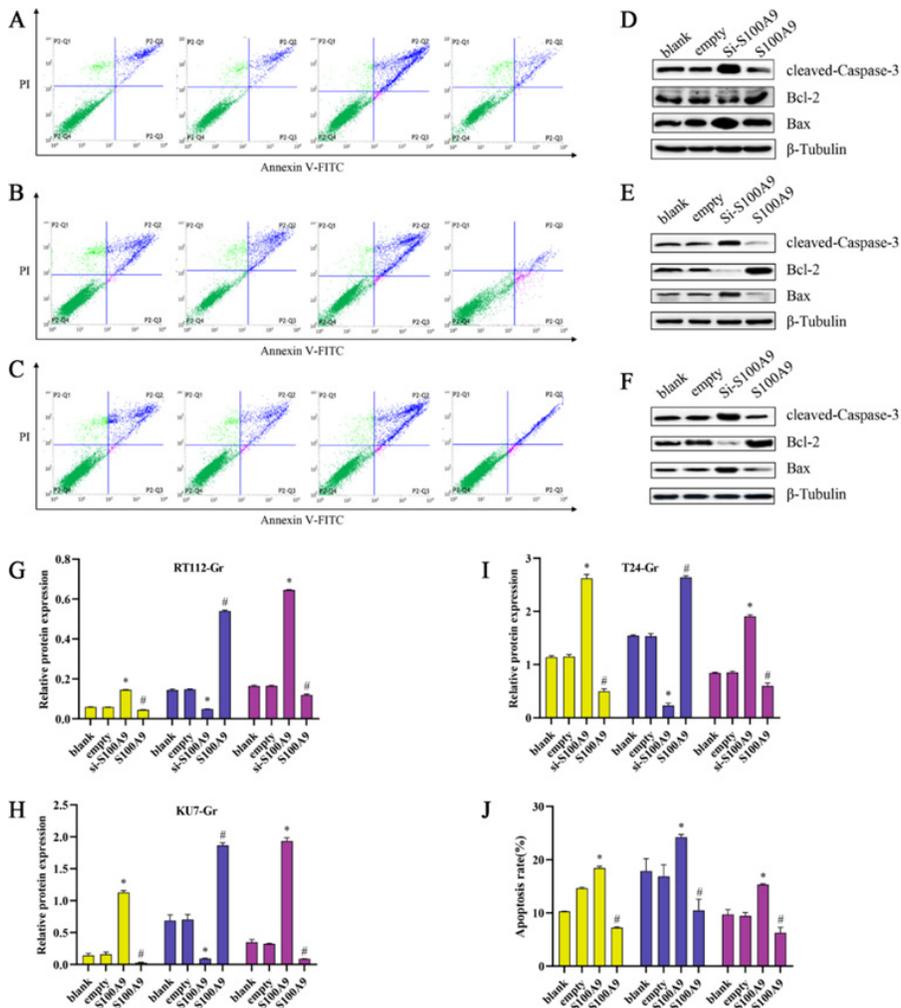

Fig. 3: The effect of S100A9 in GEM-resistant BC cells apoptosis
(A-C): The cell rate was detected by FCM and (D-J): The protein levels of cleaved caspase-3, Bcl-2 and BAX detected by Western blot assay
Note: *p<0.05 *vs.* normal cell group and #p<0.05 *vs.* empty group, (G-H) (▢): Cleaved capase-3; (▇): Bcl-2 and (▇): BAX and (J) (▢): RT112-Gr;
(▇): KU7-Gr and (▇): T24-Gr

We conducted Transwell assays to assess the migration and invasion abilities of RT112-Gr, KU7-Gr, and T24-Gr cells after S100A9 lentiviral interference. As shown in fig. 4, in KU7-Gr, T24-Gr, and RT112-Gr cells, the si-S100A9 group exhibited a significant reduction in the number of migrated and invaded cells compared to the empty control group. Conversely, in the S100A9 group, there was a significant increase in the number of migrated and invaded cells compared to the empty group. These results indicate that interfering with S100A9 expression in GEM-resistant cells can inhibit cell migration and invasion. Taken together, our findings suggest that S100A9 might hinder the therapeutic effects of GEM in GEM-resistant BC cells. This could be attributed to the upregulation of S100A9 in GEM-resistant BC cells, or possibly, GEM resistance leads to the elevated expression of S100A9. However, the exact mechanisms underlying the role of S100A9 in inhibiting the growth, migration, and invasion of GEM-resistant BC cells remain unclear. Further research is needed to elucidate these mechanisms.

To investigate whether the role of S100A9 in GEM-resistant BC cells is associated with the regulation of the PI3K/AKT/mTOR pathway, we used 10 µM LY294002 to inhibit the PI3K/AKT/mTOR pathway for 24 h. As shown in fig. 5, in RT112-Gr cells, the si-S100A9

group exhibited a significant decrease in the protein levels of p-PI3K, p-AKT, and p-mTOR compared to the empty control group. Conversely, in the S100A9 group, there was a significant increase in the protein levels of p-PI3K, p-AKT, and p-mTOR compared to the empty group. Additionally, the LY294002 group showed a significant decrease in the protein levels of p-PI3K, p-AKT, and p-mTOR compared to the empty group. However, in the S100A9+LY294002 group, the protein levels of p-PI3K, p-AKT, and p-mTOR were significantly increased compared to the S100A9 group. Similar trends were observed in KU7-Gr and T24-Gr cells. Finally, we performed MTT assays to assess cell viability after LY294002 interference in RT112-Gr, KU7-Gr, and T24-Gr cells. We found that as the intervention time of S100A9 and/or LY294002 increased, the change in cell viability gradually decreased. However, compared to the S100A9 group, the S100A9+LY294002 group showed a significant decrease in cell viability after 32 h of intervention in RT112-Gr, KU7-Gr, and T24-Gr cells. The cell viability in RT112-Gr, KU7-Gr, and T24-Gr cells decreased to <50 % within 24 h after LY294002 intervention. These findings collectively suggest that interfering with S100A9 suppresses the PI3K/AKT/mTOR pathway, thereby reducing GEM resistance in BC cells.
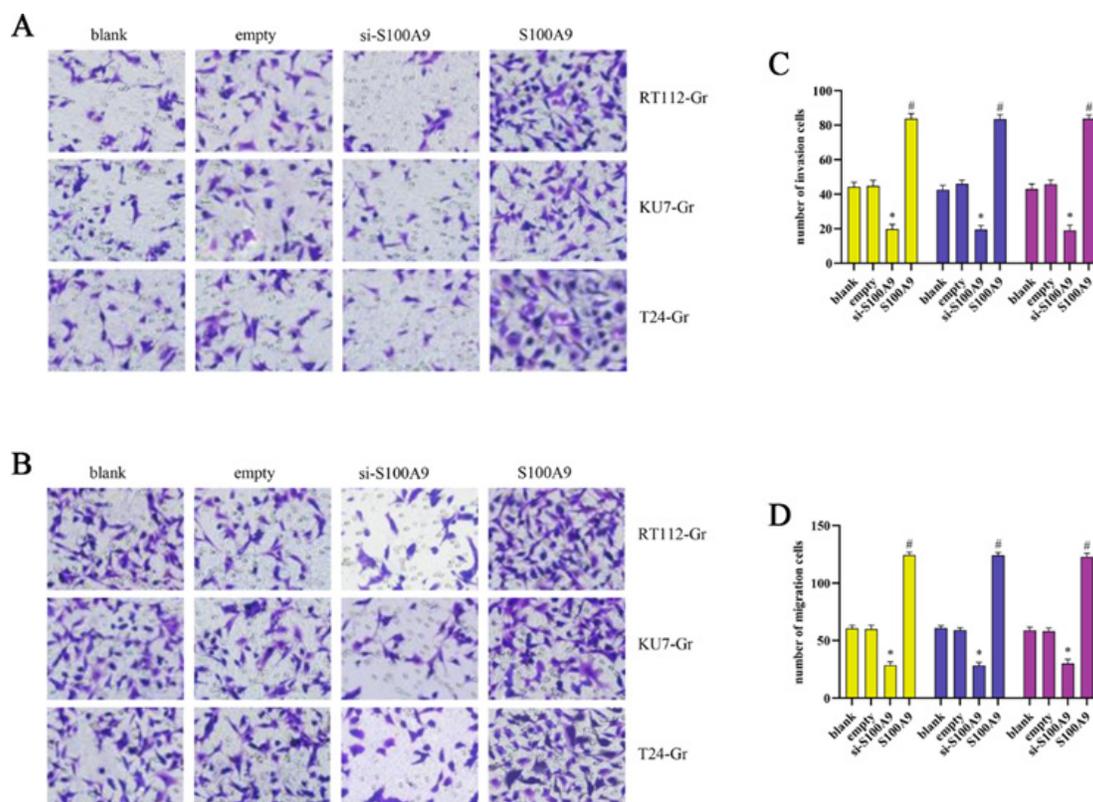

Fig. 4: The effect of S100A9 in GEM-resistant BC cells migration and invasion, (A-C): Number of invasion cells and (D): Number of migration cells
Note: *p<0.05 *vs.* normal cell group and #p<0.05 *vs.* empty group, (▢): RT112-Gr; (▢): KU7-Gr and (▢): T24-Gr
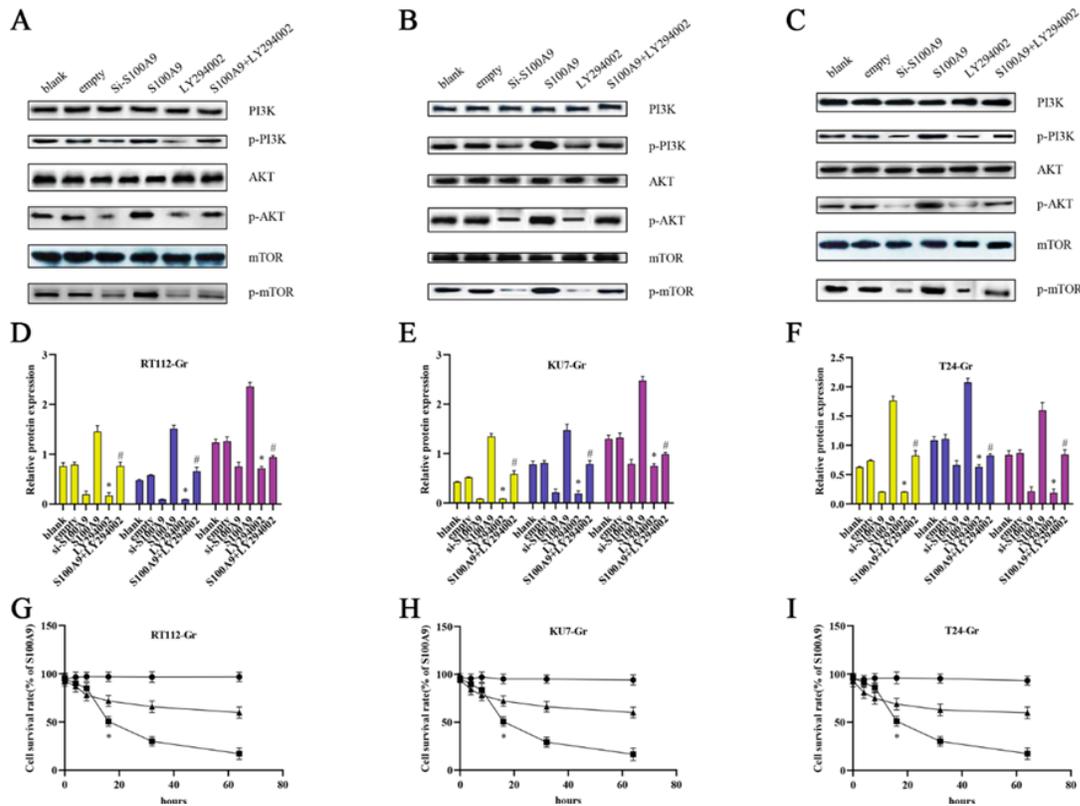
Fig. 5: S100A9 promotes phosphorylation of PI3K/AKT/mTOR pathway in GEM-resistant BC cells, (A-D): The protein levels of PI3K/Akt/mTOR pathway detected by Western blot assay in RT112-Gr; (E): The protein levels of PI3K/Akt/mTOR pathway detected by Western blot assay in KU7-Gr; (F): The protein levels of PI3K/Akt/mTOR pathway detected by Western blot assay in T24-Gr, and (G-I): MTT assay
Note: *p<0.05 *vs.* the empty group; #p<0.05 *vs.* the S100A9 group and *p<0.05 *vs.* the S100A9+LY294002 group, (D-F) (▢): p-PI3K; (▬): p-AKT and (▬): p-mTOR, (G-I) (◆): S100A9; (◆): LY294002 and (◆): S100A9+LY294002

In this study, we aimed to investigate the potential role of S100A9 in the development of GEM resistance in BC cells (RT112-Gr, KU7-Gr, T24-Gr). GEM is a commonly used chemotherapeutic agent for BC treatment, but its efficacy is often limited by the emergence of drug resistance. Understanding the underlying mechanisms of GEM resistance is essential for improving treatment strategies and patient outcomes. To address this, we employed lentivirus-mediated S100A9 overexpression and S100A9 disruptions to investigate its impact on cell viability, colony formation, migration, invasion, and apoptosis-related protein expressions in GEM-resistant BC cells. Our findings provide novel insights into the potential molecular pathways involved in GEM resistance and offer new perspectives for targeted therapies in BC.

The increased cell viability and colony formation observed upon S100A9 overexpression suggest that S100A9 may promote cell proliferation and survival in GEM-resistant BC cells. Moreover, the elevated migration and invasion abilities in S100A9-overexpressing cells indicate a potential role of S100A9 in facilitating cancer cell metastasis. Our findings are consistent with previous studies, Meng *et*

al.[19] in a review of the potential impact of circRNAs protein complexes in tumorigenesis suggests that GEM resistance is associated with migration and invasion. Wang *et al.*[20] found that NXPH4 promoted the proliferation, migration and invasion of BC cells in BC tissues. Induced GEM-resistant cell lines also showed high NXPH4 expression. This finding explains the role of NXPH4 through the mechanism of glycolysis and reactive oxygen species, and similarly to this study we validated the mechanism of action of S100A9 through the PI3K/AKT/mTOR pathway.

However, our study provides new insights into the specific role of S100A9 in GEM resistance in BC, which has not been extensively explored before. Huang *et al.*[21] found that inhibition of autophagic flux to enhance the efficiency of GEM in GEM-resistant BC cells. In addition, we have identified many studies reporting that the mechanism of action for mitigating GEM resistance is associated with autophagy[22,23]. Interestingly, it was reported that a novel protein phosphatase, Completer's Transactivated Protein 1 (CSTP1), interacts with and specifically dephosphorylates Akt at Ser473 *in vivo* and *in vitro* to arrest cell cycle progression and promote apoptosis, and that the Ser473 site of Akt is a major

cellular target of CSTP1, the expression of which is selectively down-regulated in non-invasive BC tissues[24]. This finding was further confirmed with in the present study that Akt, an intermediate in the PI3K/AKT/mTOR pathway, was phosphorylated in RT112-Gr, T24-Gr, and KU7-Gr cells, and Akt phosphorylation was attenuated after interference with S100A9.

The underlying mechanisms by which S100A9 promotes GEM resistance remain to be elucidated. In the treatment of Myelodysplastic Syndromes (MDS), previous studies have suggested that tumor escape associated with MDS can be inhibited by blocking Programmed Cell Death Protein 1 (PD-1)/Programmed Cell Death Ligand 1 (PD-L1) through activation of the PI3K/AKT/mTOR signaling pathway (36810783). Zhong et al.[25] found that S100A9 stimulated the PI3K/Akt/mTOR pathway in a rabbit vein graft model and induced Human Umbilical Vein Endothelial Cells (HUVEC) proliferation with increased viability and migration levels. In this study, after determining that S100A9 is highly expressed in GEM-resistant cells and promotes cell proliferation, we interfered with the expression level of S100A9 by lentivirus and confirmed that interfering with the expression of S100A9 had the same effect as that of LY294002 using the PI3K pathway inhibitor LY294002, and both of them inhibited the PI3K/AKT/mTOR phosphorylation signaling. Notably the activation of the PI3K/Akt/mTOR pathway and the pro-proliferative effect of S100A9 on drug-resistant cells were inhibited when S100A9 was overexpressed in the presence of LY294002. We found for the first time that interfering with S100A9 can inhibit the phosphorylation level of PI3K/Akt/mTOR pathway, which in turn reduces the proliferation, migration, and invasive ability of GEM-resistant cells, and ultimately mitigates GEM resistance, which will provide new ideas and therapeutic strategies in the clinical treatment of GEM-resistant and BC prognosis. Mediating mTOR/AKT/PI3K pathways in GEM resistance in pancreatic cancer patients in a mechanism of action study of GEM resistance[26,27]. Resistance to GEM in breast cancer cells is mainly mediated by activation of the PI3K/AKT signaling pathway[28]. However, it has not been reported that the mechanism of action of GEM resistance in BC is related to the PI3K/Akt/mTOR pathway, and the combination of LY294002 with S100A9 in the present study confirms the mechanism of action of GEM resistance in BC. The levels of p-PI3K, p-AKT and p-mTOR proteins were significantly reduced in GEM-resistant BC cells after interfering with S100A9, which ultimately inhibited cell growth, migration and invasion, promoted apoptosis and alleviated GEM resistance. It is a great novelty of the present study.

Our study has some limitations that should be addressed in future research. Firstly, we only focused on *in vitro* cell culture models, and *in vivo* experiments are needed to validate our findings in animal models. Secondly, the exact downstream targets of S100A9 mediating GEM resistance warrant further exploration. Additionally, the clinical relevance of our findings in BC patients treated with GEM remains to be investigated.

In conclusion, our study reveals that S100A9 plays a crucial role in promoting GEM resistance in BC cells. This finding sheds light on potential therapeutic targets for overcoming drug resistance in BC treatment. Targeting S100A9 may improve the efficacy of GEM-based therapies and provide new avenues for developing novel treatment strategies.

Funding:

Conflict of interests:

The authors declared no conflict of interests.

REFERENCES

1. Kaseb H, Aeddula NR. Bladder Cancer. InStatPearls. StatPearls Publishin; 2023.

2. Wang H, Mei Y, Luo C, Huang Q, Wang Z, Lu GM, *et al.* Single-cell analyses reveal mechanisms of cancer stem cell maintenance and epithelial–mesenchymal transition in recurrent bladder cancer. Clin Cancer Res 2021;27(22):6265-78.

3. Yang G, Li Z, Dong L, Zhou F. lncRNA ADAMTS9-AS1 promotes bladder cancer cell invasion, migration, and inhibits apoptosis and autophagy through PI3K/AKT/mTOR signaling pathway. Int J Biochem Cell Biol 2021;140:106069.

4. Cao HL, Liu ZJ, Huang PL, Yue YL, Xi JN. lncRNA-RMRP promotes proliferation, migration and invasion of bladder cancer *via* miR-206. Eur Rev Med Pharmacol Sci 2019;23(3):1012-21.

5. Shinoda S, Kaino S, Amano S, Harima H, Matsumoto T, Fujisawa K, *et al.* Deferasirox, an oral iron chelator, with gemcitabine synergistically inhibits pancreatic cancer cell growth *in vitro* and *in vivo*. Oncotarget 2018;9(47):28434.

6. Mun JY, Baek SW, Jeong MS, Jang IH, Lee SR, You JY, *et al.* Stepwise molecular mechanisms responsible for chemo resistance in bladder cancer cells. Cell Death Discov 2022;8(1):450.

7. Wang S, Song R, Wang Z, Jing Z, Wang S, Ma J. S100A8/A9 in inflammation. Front Immunol 2018;9:1298.

8. Willers M, Ulas T, Völlger L, Vogl T, Heinemann AS, Pirr S, *et al.* S100A8 and S100A9 are important for postnatal development of gut microbiota and immune system in mice and infants. Gastroenterology 2020;159(6):2130-45.

9. Gao F, Xu Q, Tang Z, Zhang N, Huang Y, Li Z, *et al.* Exosomes derived from myeloid-derived suppressor cells facilitate castration-resistant prostate cancer progression *via* S100A9/circMID1/miR-506-3p/MID1. J Transl Med 2022;20(1):346.

10. Kim WT, Kim J, Yan C, Jeong P, Choi SY, Lee OJ, *et al.* S100A9 and EGFR gene signatures predict disease progression in muscle invasive bladder cancer patients after chemotherapy. Ann Oncol 2014;25(5):974-9.

11. Liu L, Liu S, Deng P, Liang Y, Xiao R, Tang LQ, *et al.* Targeting the IRAK1–S100A9 axis overcomes resistance to paclitaxel in nasopharyngeal carcinoma. Cancer Res 2021;81(5):1413-25.

12. Chen H, Huang J, Chen C, Jiang Y, Feng X, Liao Y, *et al.* NGFR increases the chemosensitivity of colorectal cancer cells by enhancing the apoptotic and autophagic effects of 5-fluorouracil *via* the activation of S100A9. Front Oncol 2021;11:652081.

13. Tanigawa K, Tsukamoto S, Koma YI, Kitamura Y, Urakami S, Shimizu M, *et al.* S100A8/A9 induced by interaction with macrophages in esophageal squamous cell carcinoma promotes the migration and invasion of cancer cells *via* Akt and p38 MAPK pathways. Am J Pathol 2022;192(3):536-52.

14. Zhang Y, Liu F, Feng Y, Xu X, Wang Y, Zhu S, *et al.* circRNA circ_0006156 inhibits the metastasis of prostate cancer by blocking the ubiquitination of S100A9. Cancer Gene Ther 2022;29(11):1731-41.

15. Moradpoor R, Gharebaghian A, Shahi F, Mousavi A, Salari S, Akbari ME, *et al.* Identification and validation of stage-associated PBMC biomarkers in breast cancer using MS-based proteomics. Front Oncol 2020;10:1101.

16. Yi W, Zhu R, Hou X, Wu F, Feng R. Integrated analysis reveals S100a8/a9 regulates autophagy and apoptosis through the MAPK and PI3K-AKT signaling pathway in the early stage of myocardial infarction. Cells 2022;11(12):1911.

17. Wen L, Ding Y, Chen X, Tian K, Li D, Liang K, *et al.* Influences of S100A8 and S100A9 on proliferation of nasopharyngeal carcinoma cells through PI3K/akt signaling pathway. Biomed Res Int 2021;2021:9917365.

18. Fan ZP, Peng ML, Chen YY, Xia YZ, Liu CY, Zhao K, *et al.* S100A9 activates the immunosuppressive switch through the PI3K/Akt pathway to maintain the immune suppression function of testicular macrophages. Front Immunol 2021;12:743354.

19. Meng X, Xiao W, Sun J, Li W, Yuan H, Yu T, *et al.* circPTK2/PABPC1/SETDB1 axis promotes EMT-mediated tumor metastasis and gemcitabine resistance in bladder cancer. Cancer Lett 2023;554:216023.

20. Wang D, Zhang P, Liu Z, Xing Y, Xiao Y. NXPH4 promotes gemcitabine resistance in bladder cancer by enhancing reactive oxygen species and glycolysis activation through modulating NDUFA4L2. Cancers 2022;14(15):3782.

21. Huang Z, Wang T, Xia W, Li Q, Chen X, Liu X, *et al.* Oblongifolin C reverses GEM resistance *via* suppressing autophagy flux in bladder cancer cells. Exp Ther Med 2020;20(2):1431-40.

22. Yang X, Yin H, Zhang Y, Li X, Tong H, Zeng Y, *et al.* Hypoxia-induced autophagy promotes gemcitabine resistance in human bladder cancer cells through hypoxia-inducible factor 1α activation. Int J Oncol 2018;53(1):215-24.

23. Yin L, Liu S, Li C, Ding S, Bi D, Niu Z, *et al.* CYLD downregulates livin and synergistically improves gemcitabine chemosensitivity and decreases migratory/invasive potential in bladder cancer: The effect is autophagy-associated. Tumor Biol 2016;37(9):12731-42.

24. Zhuo DX, Zhang XW, Jin B, Zhang Z, Xie BS, Wu CL, *et al.* CSTP1, a novel protein phosphatase, blocks cell cycle, promotes cell apoptosis, and suppresses tumor growth of bladder cancer by directly dephosphorylating Akt at Ser473 site. PLoS One 2013;8(6):e65679.

25. Zhong X, Xie F, Chen L, Liu Z, Wang Q. S100A8 and S100A9 promote endothelial cell activation through the RAGE-mediated mammalian target of rapamycin complex 2 pathway. Mol Med Rep 2020;22(6):5293-303.

26. Guo Y, Wu H, Xiong J, Gou S, Cui J, Peng T. miR-222-3p-containing macrophage-derived extracellular vesicles confer gemcitabine resistance *via* TSC1-mediated mTOR/AKT/PI3K pathway in pancreatic cancer. Cell Biol Toxicol 2023;39(4):1203-14.

27. Lan CY, Chen SY, Kuo CW, Lu CC, Yen GC. Quercetin facilitates cell death and chemo sensitivity through RAGE/PI3K/AKT/mTOR axis in human pancreatic cancer cells. J Food Drug Anal 2019;27(4):887-96.

28. Yang XL, Lin FJ, Guo YJ, Shao ZM, Ou ZL. Gemcitabine resistance in breast cancer cells regulated by PI3K/AKT-mediated cellular proliferation exerts negative feedback *via* the MEK/MAPK and mTOR pathways. Onco Targets Ther 2014;7:1033-42.